URSI-B EMTS 2025, Bologna, 23–27 June

Reusing Submatrix Calculations in Array Decomposition Method for Finite Arrays with Electrically Connected Elements

Lucas Åkerstedt(1)*, Harald Hultin(1)(2), and B. L. G. Jonsson(1)
(1) KTH Royal Institute of Technology, Stockholm, Sweden, lucasak@kth.se
(2) Saab Surveillance, 175, 41 Järfälla, Sweden

Abstract

The finite partial translation symmetry apparent in array antennas can be exploited for effective calculation of the Method of Moments (MoM) impedance matrix. With a geometrical array decomposition built on nine subdomain components, the obtained MoM impedance matrix inherits a partial block Toeplitz structure, which enables fast calculation time and reduces memory allocation. In this paper, we further improve the calculation time by reusing already calculated submatrices of the MoM impedance matrix. By identifying corresponding elements between the nine components, already calculated submatrices can be extracted to create submatrices previously deemed as necessary to calculate. The reusing strategy reduces the number of submatrix calculations to perform from $\mathscr{O}(N_xN_y)$ to $\mathscr{O}(N_x+N_y)$, of a part of the impedance matrix, for an $N_x \times N_y$ array.

1 Introduction

Accurate full-wave calculations of electrically large array antennas using ordinary MoM are well-known to be computationally demanding. The computational challenges addressed here focus on calculating the MoM impedance matrix and solving the MoM equation system. For ordinary MoM, building the MoM impedance matrix scales as $\mathscr{O}(N^2)$, where N is the number of triangle edge elements necessary to constitute an accurate current representation on the discretized object. To obtain accurate calculations of electrically large array antennas, the necessary memory allocation for the MoM impedance matrix exceeds that of the memory typically available in personal computers, limiting the method to super-computers only.

Several methods for reducing the computational demands of ordinary MoM while exploiting the translation symmetry of the array antenna have been successfully employed [1–5]. By partitioning the array into subdomains, only a fraction of submatrices (corresponding to these inter-subdomain calculations) are necessary to represent the complete MoM impedance matrix. In [3, 6, 7], this methodology has been extended to the case of array antennas with electrically connected elements.

Both of the methods in [3, 6] rely on an array representation consisting of nine subdomain components. In MoM, only the interior edges of a meshed surface are considered for the current representation. Subsequently, the non-periodic part like the edge region of a ground plane is treated differently, motivating the nine components representation. Of these components, the center component constitutes the array element and its associated ground plane, whereas the surrounding components constitute margin or modified elements at the boundary of the array.

In [6], the MoM impedance matrix is constructed by only calculating the necessary impedance relations between components. This procedure yields a MoM impedance matrix where the largest part (antenna element coupling) has a multilevel block Toeplitz structure. The margin-to-elements impedance relation becomes a 1-level block Toeplitz structure. Similarly, the margin-to-margin coupling yields partly a 1-level block Toeplitz structure and partly a 2-level block Toeplitz structure.

Using the algorithm from [6] in its current state, a large fraction of the time is spent on calculating the impedance relation between the margin and the elements. In this paper, we focus on reducing this calculation time. A majority of the margin-to-element submatrix calculations can be reused from the impedance relation among the array elements. This methodology is, however, limited to array antennas where the margin component is 'similar' to parts of the array element component (the exact requirements are presented in Section 3). Upon reusing the calculations, the calculation time of the impedance relation between the margin and the array elements is reduced from $\mathscr{O}(N_xN_y)$ to $\mathscr{O}(N_x+N_y)$ (for an $N_x \times N_y$ array antenna). The modification accelerates the calculation of array antennas with elements placed on top of an extended finite ground plane.

2 MoM with Array Partitioning

The MoM algorithm in [6] assumes that the array antenna can be built from the array components obtained using complete partitioning (one array element component and eight margin components). These nine array components serve as basic building blocks. In Fig 1(a), an example of nine array components is displayed, and how the components' edge elements share associated triangles. In Fig. 1(b), a 4×6 array, constructed using the nine array components is displayed as an example.

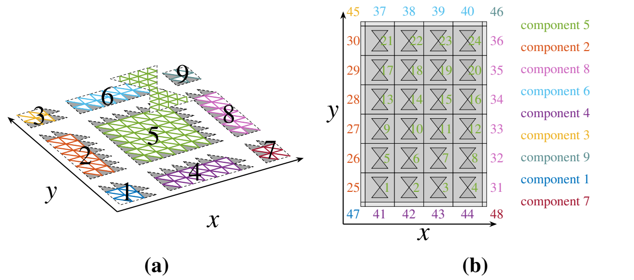

Figure 1. (a) Exploded view of mesh partitioned into nine subdomains to create the array element and margin components. (b) A 4×6 array constructed using element and margin components. (a) and (b) are color matched.

Each part of the array is described by an array component and an offset. Subsequently, the MoM impedance matrix is obtained as a block matrix, where each block is the MoM impedance relation between two parts, here denoted as $Z_{ij}\in\mathbb{C}^{N_i\times N_j}$, where N_i and N_j are the number of edge elements in parts i and j, respectively. The elements of the submatrix Z_{ij} are calculated using the standard MoM impedance formulation

$$z_{mn}=\frac{-\mathrm{j}\eta}{k}\int_{T_n}\int_{T_m}\nabla'_S\cdot\boldsymbol{f}_n(\boldsymbol{r}')G(\boldsymbol{r},\boldsymbol{r}')\nabla_S\cdot\boldsymbol{f}_m(\boldsymbol{r})\mathrm{d}S\mathrm{d}S' \\ +\mathrm{j}k\eta\int_{T_n}\int_{T_m}G(\boldsymbol{r},\boldsymbol{r}')\boldsymbol{f}_n(\boldsymbol{r}')\cdot\boldsymbol{f}_m(\boldsymbol{r})\mathrm{d}S\mathrm{d}S', \tag{1}$$

where m are the edge indices of part i, n are the edge indices of part j, j is the imaginary unit, η is the impedance of the medium, k is the wave number, $\boldsymbol{f}$ is the basis function (typically the RWG element), T_n are the plus and minus triangles associated with edge n ($T_n=T_n^{+}+T_n^{-}$), and $G(\boldsymbol{r},\boldsymbol{r}')$ is the Green function.

By ordering the parts as indicated in Fig. 1(b) prior to calculating all impedance relations Z_{ij}, the MoM impedance matrix is obtained as

$$Z=\begin{bmatrix}A & B^T\\ B & C\end{bmatrix}, \tag{2}$$

where matrix A corresponds to the impedance relation among the antenna elements, matrix B corresponds to the impedance relation between the margin and elements, and where matrix C corresponds to the impedance relation among the margin parts.

Since the Green function $G(\boldsymbol{r},\boldsymbol{r}')$ is translation invariant, many submatrices in A, B, and C are identical. As a result, matrix A inherits a multilevel block Toeplitz structure, resulting in a small number of unique submatrices. In Fig. 2(a), a visualization of matrix A is depicted corresponding to the 4×6 array displayed in Fig. 1(b). Exploiting the first level of block Toeplitz structure yields the submatrices depicted in Fig. 2(b), whereas exploiting the second level of Toeplitz structure and the symmetry of the matrix yields the only necessary submatrix calculations to represent the complete matrix A, as depicted in Fig. 2(c).

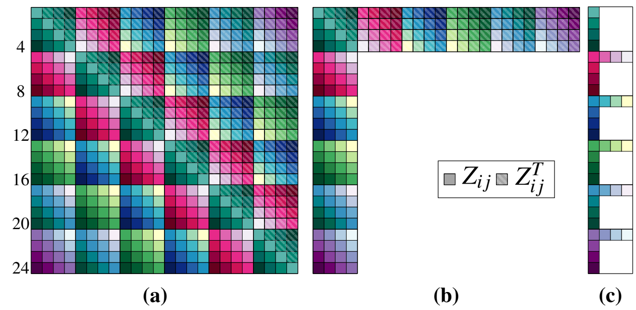

Figure 2. (a) Submatrix blocks of matrix A, where blocks of the same color indicates identical submatrices. (b) First level of block Toeplitz structure. (c) Second level of block Toeplitz structure and using $A=A^T$.

A block Toeplitz structure is also found in matrix B, representing margin-to-element coupling. These simplifications are, however, not available to the same extent as in matrix A. In Fig. 3(a), the structure of matrix B is illustrated, and in Fig. 3(b), only the necessary submatrix calculations are shown.

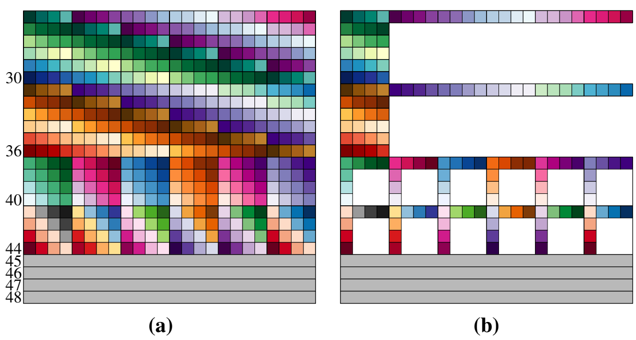

Figure 3. (a) Submatrix blocks of matrix B, where blocks of the same color indicates the same submatrix. Grey areas indicates unique submatrices. (b) First level of block Toeplitz structure.

The matrix C also inherits some block Toeplitz structure [6]. To solve the MoM equation system $ZI=V$, the Schur complement is used on (2), which yields

$$I_1=U-FI_2,\quad I_2=-(C-BF)^{-1}BU,\quad I=\begin{bmatrix}I_1\\ I_2\end{bmatrix}. \tag{3}$$

Here, U and F are obtained through solving the equation system

$$A\begin{bmatrix}U & F\end{bmatrix}=\begin{bmatrix}V_1 & B^T\end{bmatrix},\quad V=\begin{bmatrix}V_1\\ 0\end{bmatrix}. \tag{4}$$

Excitations are only in the element parts, motivating the form of V. From (3) and (4), it is clear that the size of matrix B impacts the solution time. In [7], fast and efficient solutions to (4) are discussed.

The above results in Fig. 2 and 3 show that for a general $N_x \times N_y$ array, matrix A requires $2N_xN_y - N_x - N_y + 1$ submatrix calculations, whereas matrix B requires $12N_xN_y - 2N_x - 2N_y$. The submatrix calculations of B are often faster to compute than submatrices in A since the margin parts typically contain fewer triangular edge elements. However, using the MoM algorithm from [6] for arrays with a large number of elements and with broader margin components, the majority of the submatrix calculation time is spent on calculating matrix B.

3 Reusing Submatrix Calculations

The submatrices illustrated in Fig. 3(b) are unique, meaning that no other submatrix in the MoM impedance matrix Z is the same as the highlighted submatrices. However, if the margin components are *similar* to the element component, certain rows of the submatrices from matrix A can be extracted to yield submatrices that are the same as the majority of the unique submatrices in Fig. 3(b). For planar arrays with a ground plane, the margin components are frequently similar to parts of the element component, as seen in Fig. 1.

Consider a submatrix calculation between a margin and an array element, a distance D apart, as Fig. 4(a) suggests. The calculation yields the submatrix Z_{ij}. If the margin part has corresponding edge elements in the array element component, the submatrix Z_{ij} can be obtained from the already calculated submatrix describing the coupling between two array elements, a distance D apart, as Fig. 4(b) suggests. If all the edge elements of the margin component have corresponding edge elements within the array element component, the margin component is here defined to be similar to the array element component.

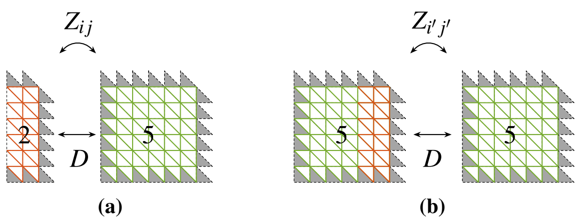

Figure 4. (a) Margin to element part submatrix calculation. (b) Element to element part submatrix calculation, where the margin component's corresponding edge elements are highlighted in red.

By displacing a margin component's edge elements D_u into the element component, each corresponding (overlapping) edge element of the element component can be identified, where D_u is either the width or the length of the element component. Here, it is crucial to identify if the element component's edge elements associated plus and minus triangles are oriented as the margin component's elements.

The submatrix Z_{ij} associated with a Fig. 4(a) type of display can be calculated as

$$Z_{ij} = TEZ_{i'j'}, \tag{5}$$

where $Z_{i'j'}$ is the corresponding array element-to-element submatrix calculation, e.g, Fig. 4(b). Here, E is defined by

$$E = \begin{bmatrix} \hat{\boldsymbol{e}}_{c(1)} & \cdots & \hat{\boldsymbol{e}}_{c(N_m)} \end{bmatrix}^T \in \mathbb{N}^{N_m \times N_e}, \tag{6}$$

where $\hat{\boldsymbol{e}}_k$ is the kth column of the identity matrix, $[c(1), \ldots, c(N_m)]$ are the edge indices to the corresponding edge elements in the element component, N_e is the number of edge elements in the element component, and where N_m is the number of edge elements in the margin component. The matrix T is obtained as

$$T = \operatorname{diag}(t(1), \ldots, t(N_m)) \in \mathbb{Z}^{N_m \times N_m}, \tag{7}$$

where $t(k) = 1$ if the plus and minus triangles of the margin component edge element k are oriented as the plus and minus triangle of its corresponding edge element, and $t(k) = -1$ if otherwise.

In Fig. 5, strategies for finding element component submatrix calculations to be reused with (5) are displayed.

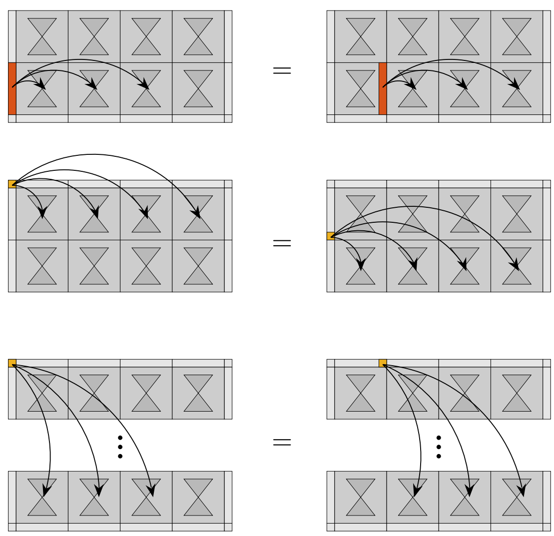

Figure 5. The left highlighted region's coupling to the array elements are the same as the coupling indicated to the right.

The above described strategy strongly reduces the necessary number of submatrices to calculate. In Fig. 6, the remaining submatrix calculations are depicted for the 4×6 array in Fig. 1. For the general $N_x \times N_y$ array matrix B now instead requires $4(N_x + N_y)$ calculations. This is a reduction from $\mathcal{O}(N_xN_y)$ to $\mathcal{O}(N_x + N_y)$.

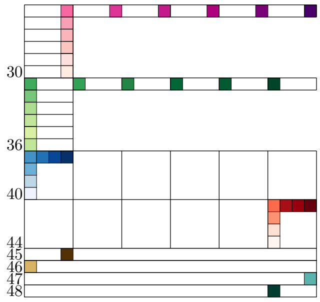

Figure 6. Necessary submatrix calculations to construct the complete matrix B with the reusing strategy, for the 4×6 array case.

4 Numerical Example

In this example, the Embedded Element Pattern (EEP) of two 15×15 arrays is calculated for a frequency $f_0 = 18\,\mathrm{GHz}$. The array element used in both arrays is a fully metallic BoR element, as can be seen in the inset if Fig. 7. What separates the two arrays is the size of the margin ($\lambda/2$ and $\lambda/10$) of the two array representations, α and β, visualized in the inset of Fig. 7. In Fig. 7, the embedded element pattern of the corner and center element is plotted, for the two arrays. Calculating matrix B for the two array cases, α and β, constitutes 4.3%, and 1.1% of their respective total MoM impedance calculation time.

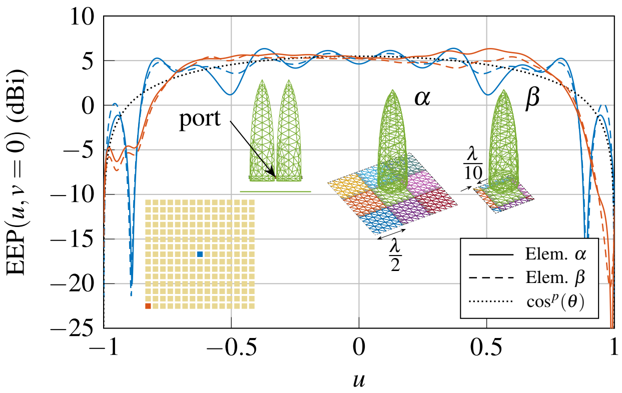

Figure 7. Embedded element patterns plotted for two cases of margins used, and a $\cos^p(\theta)$ pattern where $p = 0.75$. The blue (red) plot corresponds to the center (corner) EEP.

5 Conclusion

In this paper, we have proposed a strategy for reusing submatrix calculations from matrix A to reduce the necessary submatrix calculations to construct matrix B. The method relies on identifying edge elements in the margin components corresponding to edge elements in the element component. With the reusing strategy, the number of submatrix calculations to perform to construct matrix B now scales as $\mathcal{O}(N_x + N_y)$, which is a better scaling than the number of necessary calculations to construct matrix A, motivating the use of the nine components approach. Additionally, the reusing strategy can also be used on matrix C.

6 Acknowledgements

This work was supported by the Swedish Foundation for Strategic Research (ID20-0004), the Strategic Innovation Program Smarter Electronics System (2022-00833), by Vinnova, Formas, and the Swedish Energy Agency, and the Swedish Research Council's Research Environment grant (SEE-6GIA 2024- 06482) for research on sixth-generation wireless systems (6G).

References

[1] E. Bleszynski, M. Bleszynski, and T. Jaroszewicz, "Block-Toeplitz fast integral equation solver for large finite periodic and partially periodic antenna arrays," in *2003 IEEE Topical Conference on Wireless Communication Technology*, 2003, pp. 428–429.

[2] R. Kindt, K. Sertel, E. Topsakal, and J. Volakis, "Array decomposition method for the accurate analysis of finite arrays," *IEEE Transactions on Antennas and Propagation*, vol. 51, no. 6, pp. 1364–1372, 2003.

[3] M. Brandt-Møller, M. Mattes, O. Breinbjerg, M. Zhou, and E. Jørgensen, "Extended Higher-Order Array Decomposition Method for Fully Populated or Thinned Array Antennas and Scatterers With Connected Elements," *IEEE Transactions on Antennas and Propagation*, vol. 72, no. 5, pp. 4454–4464, 2024.

[4] Y. Zhao, S. Xiang, J. Han, and L. Li, "Hierarchical Pattern Exploitation for Efficient Electromagnetic Analysis of Finite Periodic Array," *IEEE Transactions on Antennas and Propagation*, vol. 70, no. 12, pp. 12 417–12 422, 2022.

[5] W. Xiang, T. Xiong, W.-B. Lu, W. Yang, and Z.-G. Liu, "New Accurate Subentire-Domain Basis Functions Method for the Analysis of Large-Scale Finite Periodic Structures with Electrically Connected Cells," *IEEE Transactions on Antennas and Propagation*, vol. 67, no. 3, pp. 2017–2022, 2019.

[6] L. Åkerstedt, H. Hultin, and B. L. G. Jonsson, "Array Decomposition Method for Array Antennas with Electrically Connected Elements Using RWG-like Elements," 2024, in preperation.

[7] H. Hultin, L. Åkerstedt, and B. L. G. Jonsson, "Performance of Accelerated MoM for Connected Arrays," 2024, in preperation.